ELSEVIER

Applied Surface Science 92 (1996) 519–525

applied surface science

High quality quantum dots fabricated by molecular beam epitaxy

Chien-Ping Lee *, Der-Cherng Liu

Department of Electronics Engineering and Institute of Electronics, National Chiao Tung University, Hsin Chu 30039, Taiwan, ROC

Received 12 December 1994; accepted for publication 4 March 1995

Abstract

Damage free quantum dots have been fabricated directly using molecular beam epitaxy. Excellent photoluminescence has been obtained and is attributed to the absence of the non-radiative recombination centers and the enhanced oscillator strength for exciton recombination due to the confinement of quantum dots. The size variation of the quantum dots has been estimated from the width of the emission peak of low temperature photoluminescence (PL). A variation of only ± 10 Å is obtained. The existence of the quantum dots has also been verified directly from the image of the dots using atomic force microscopy. The image sizes of the quantum dots agree with that estimated from the PL blue shift.

1. Introduction

Semiconductor "quantum dot" structures have attracted a lot of attention recently for their enhanced optical properties [1,2], and for potential applications in ultimate quantum devices. However to obtain such structures requires difficult material growth and processing techniques. Several methods have been reported to have resulted in quantum dot structures. These techniques usually utilize electron beam (e-beam) lithography or holographic lithography, subsequent wet or dry etching processes and/or regrowth [3–7]. Although quantum effects have been reported, most of the approaches used are far from ideal. One of the main drawbacks is the existence of a high density of surface states due to the etching and regrowth process resulting in enhancement of non-radiative recombinations and degradation of optical properties.

In this paper a new technique for semiconductor quantum dot fabrication is presented. The quantum dots are obtained in a single molecular beam epitaxy (MBE) growth run. The technique utilizes the property of different thermal desorption rates between different materials to create nonuniform thermal evaporation in a thin epilayer to result in quantum dots. Because it is an in situ process and the regrowth is performed immediately after thermal etching, the "surface states" problem is avoided. Furthermore, since the quantum dots are obtained by thermal etching, no lithography step is needed.

2. Experimental

When a semiconductor sample is heated to high temperatures, the atoms are desorbed or evaporated from the sample. The evaporation rates of materials depend on the thermal activation energy, E_a. If a thin epilayer is covered by a incomplete layer with a higher E_a and is then heated to high temperatures,

* Corresponding author. Fax: +886 35 713403; e-mail: cplee@cc.nctu.edu.tw.

SSDI 0169-4332(95)00288-X

the upper layer would act as a mask and the layer underneath but not covered by the upper layer would evaporate and result in an island structure. If the layer underneath is thin enough and the islands are small enough, quantum dots are obtained. The procedure for producing the quantum dots is shown in Fig. 1. After the growth of a thin quantum well, a thin layer with a high E_a is deposited on the surface of the quantum well. Then the growth is interrupted and the substrate temperature is raised to cause "thermal etching" or "thermal evaporation" for the underlying quantum well. If the material and the thickness of the upper layer is chosen so that it forms small islands, the islands would behave like a mask during "thermal etching". After etching, another layer with a wider bandgap is deposited and the islands that are not evaporated become quantum dots.

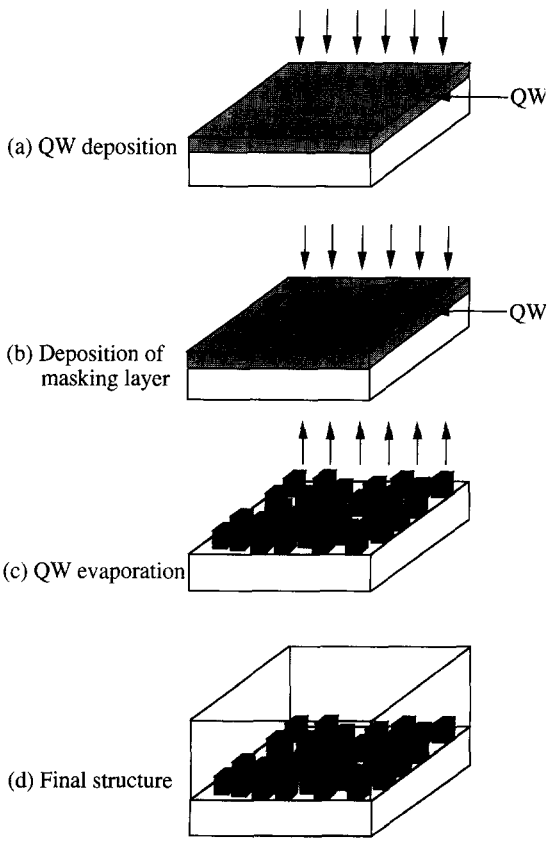

Fig. 1. The growth procedure of the quantum dots.

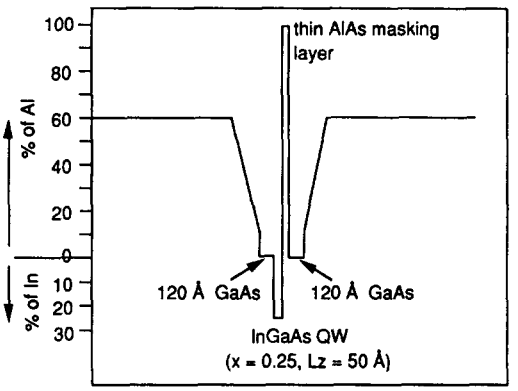

Fig. 2. Schematic layer structure used in this study. Thermal etching was performed after the deposition of the thin AlAs to form the quantum dots.

The layer structure used to prepare the quantum dots is shown in Fig. 2. A 50 Å $In_xGa_{1-x}As$ ($x = 0.25$) strained quantum well is sandwiched between two 120 Å GaAs barriers in a graded-index separate-confinement heterostructure (GRIN-SCH). Above the quantum well a very thin AlAs layer was grown. The thickness of this layer was chosen to be thin enough and the growth temperature low enough so that it formed small islands after growth. These islands then served as masks for the subsequent thermal etching of the InGaAs layer. Since InGaAs evaporates at a much lower temperature than that of AlAs, the InGaAs layer not covered by the AlAs islands was thermally etched when the substrate temperature was raised to a proper etching temperature. After thermal etching, the InGaAs left behind formed quantum dots. The GaAs layer grown afterwards then formed the potential barrier surrounding the quantum dots. This technique is very simple and the quantum dots can be easily incorporated in many heterostructure devices. As an example, the structure shown in Fig. 2 would be an ideal structure for quantum dot lasers. More importantly, the quantum dots fabricated this way do not have any surface states caused by process related damages. Detailed fabrication procedure has been reported in Ref. [8]. Recently there have been several reports on growing damage free InAs or InGaAs quantum dots on GaAs [9–11]. But in those techniques, one usually does not have much control on the thickness or the z dimension of the dots.

3. Optical characterization

Low temperature photoluminescence was used to examine the amount of blue shift caused by the lateral confinement of the quantum dots and the quality of the dots. The excitation source was the 5145 Å line of an Ar ion laser. Fig. 3a shows the 11 K PL spectrum of a sample which had a AlAs mask layer with an average thickness of half a monolayer (0.5 ML). The thermal etching temperature was 670°C. The long wavelength peak in the spectrum is due to the InGaAs quantum well, which was grown below the quantum dot layer as a reference. This quantum well, which is 2000 Å below the quantum dots, had exactly the same structure as that shown in Fig. 1 which was used to prepare the quantum dots except no thermal etching was performed after the thin AlAs growth. The emission peak of the quantum dots had a ~ 73 meV energy shift from that of the InGaAs quantum well reference. If these dots are assumed to be square-shaped, the average size of the dots is 108 by 108 Å. These dimensions are much smaller than what any lithographic technique can make [12–16]. Since only half a monolayer of AlAs was deposited, if we assume the AlAs islands had a thickness of one monolayer [17], the area that was covered by the AlAs mask and eventually turned into quantum dots is half of the total surface area. Based on the average size of the quantum dots, it can then be estimated that the areal density of the quantum dots is 5×10^{11} cm^{-2}. Taking into account the dots' thickness, we get a total volume density of 10^{18} cm^{-3} for the quantum dots. For most device applications, it is important to have a high density for the quantum dots because only a few electrons (or holes) are confined in each dot. The number we obtained here is certainly high enough for many such applications. The size of the quantum dots could be changed by using different thickness for the AlAs mask and different thermal etching temperature. Fig. 3b shows the 11 K PL spectrum for a sample with 3.5 monolayers of AlAs as the mask and a etching temperature of 690°C. The blue shift of the emission peak due to quantum dots formation is ~ 24 meV. The estimated lateral dimensions of the dots based on this energy shift are 215 by 215 Å.

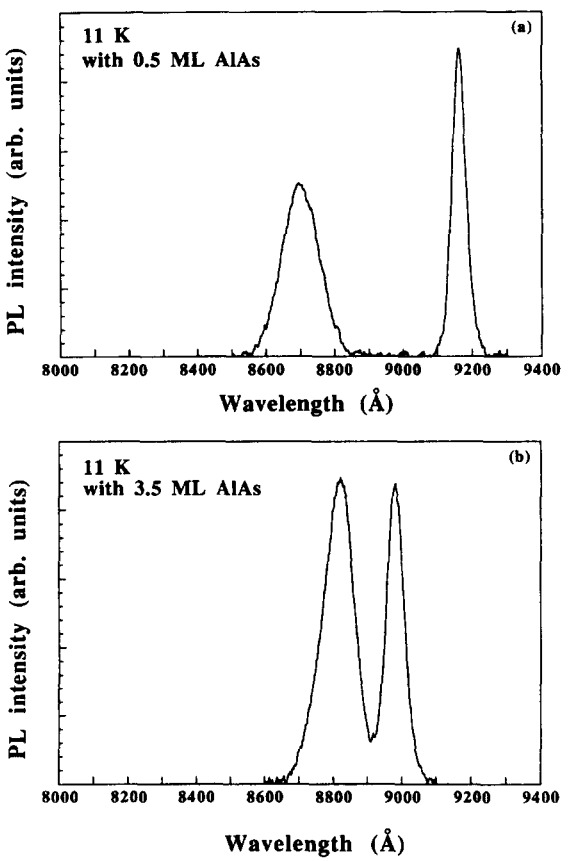

Fig. 3. 11 K PL spectra of the samples with quantum dots and quantum wells references. In (a), the thin AlAs layer was 0.5 monolayer thick and the quantum dots were obtained after 670°C thermal etching. In (b), AlAs of 3.5 monolayers was deposited and thermal etching was performed at 690°C.

From Fig. 3, it is noticed that the intensity of the emission peak from quantum dots is very strong. The peak's integrated intensity is higher than that of the reference InGaAs quantum well. Although the InGaAs quantum well is 2000 Å deeper than the quantum dots, the attenuation of the Ar laser light due to this additional thin layer should not be enough to account for this difference. Besides, the total volume of the quantum dots is smaller than that of the quantum well because part of the InGaAs layer has been evaporated away. For the case with half of a monolayer of AlAs as the evaporation mask, the largest possible total volume for the quantum dots is only half that of the InGaAs quantum well. So, it is clear that the radiative recombination efficiency per unit volume is much higher for quantum dots than that for quantum wells. This increase in emission

intensity can be explained by the enhanced oscillator strength for exciton recombination due to the confinement of excitons to the small quantum dots [18]. There are theoretical analyses, however, showing the electron relaxation from the excited state to the ground state is greatly hindered in quantum dots resulting in low luminescence efficiency [19,20]. The high PL intensity observed from our dots obviously does not agree with the theoretical prediction. Recently other groups have also reported very high PL emission from their quantum dots [10,21]. So there must be some relaxation mechanism for the excited carriers. Vurgaftman and Singh have recently calculated the carrier relaxation process using the Monte Carlo method [22]. They have found that the scattering of electrons and holes in quantum dots can significantly reduce the carrier relaxation time. As indicated in their paper, this may explain the experimentally observed high luminescence intensity from quantum dots.

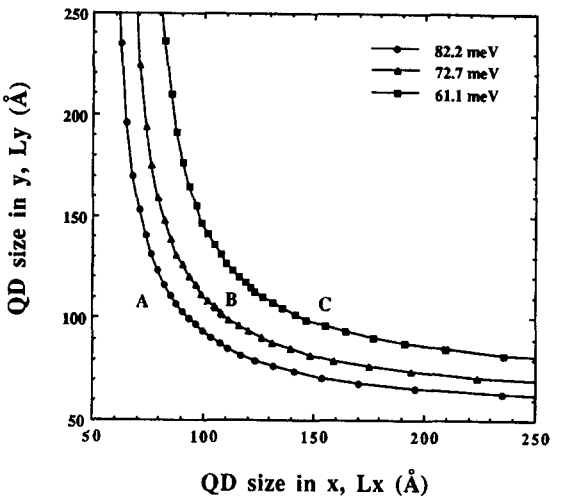

Fig. 4. Calculated lateral quantum dot dimensions based on square potential well model. The curves were calculated from the amount of the blue shift from that of the reference quantum well shown in Fig. 3a. The three curves correspond to the sizes of the quantum dots at the peak and the two middle points of the emission peak.

4. Uniformity

The size variability is an important issue for quantum dot fabrication. We have estimated the size variation of our quantum dots from the PL spectrum assuming the width of the PL emission peak is solely caused by the variation of the quantum dot sizes. Because the amount of the blue shift is due to the quantum confinement of the dots, the lateral dimensions, L_x and L_y (assuming they have rectangular shapes), can be calculated based on the energy shift. Fig. 4 shows the calculated L_x and L_y for three different energies, which correspond to the peak position and the two side positions (at half width) of the emission peak shown in Fig. 3a. The calculation was done based on square potential well model, and for simplicity, no Coulomb interaction between electrons and holes was considered. If we assume the dots are square, i.e., $L_x = L_y$, the peak position gives a dot size of 108 by 108 Å. The width of the PL peak gives a standard deviation of only ± 10 Å. It should be kept in mind, however, that the sizes and the variation of the quantum dots were estimated without considering the Coulomb interaction between the electron and the hole. Bryant has indicated in his theoretical analysis that the binding energy for an exciton in a quantum box is less sensitive to size variation as expected from pure quantum confinement [14]. In other words, the actual size variation should be larger than that estimated without Coulomb interaction. Even this is the case, the uniformity of the dots obtained here is remarkable considering the dots are formed naturally without any lithographic patterning. Recently there have been reports on growing InAs and InGaAs quantum dots on GaAs [6,7]. The lateral size variation of those dots was in the order of $\pm 10\%$, which is similar to what we observe here. The reason given for such low size dispersion was the self-organization of the dots during growth. In our technique, the AlAs mask was grown on top of InGaAs and then the sample was brought to high temperature for thermal evaporation. The island formation is probably also self-organized to result in uniform islands.

5. Masking layer consideration

In this technique, the thickness of the AlAs mask is of crucial importance. If it is too thick, the quantum well underneath will be totally covered and subsequent thermal evaporation will not cause any

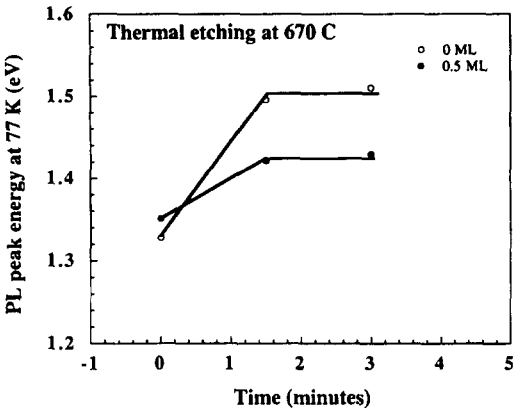

Fig. 5. Peak emission energy of PL spectra at 77 K of samples with and without 0.5 ML AlAs mask after thermal etching at 670°C.

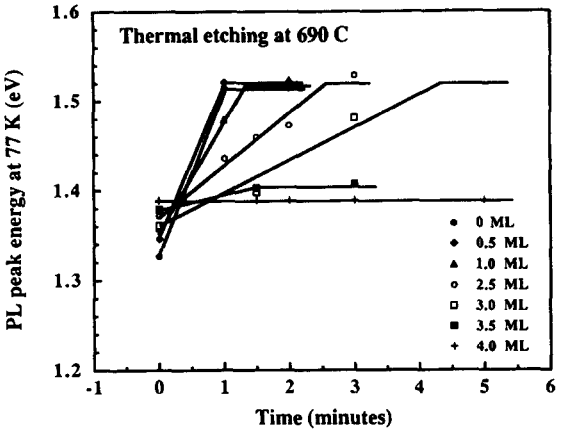

Fig. 6. Peak emission energy of PL spectra at 77 K for samples with different AlAs mask thicknesses after thermal etching at 690°C.

island formation. If it is too thin, the quantum well layer will be totally evaporated away and also cannot form any quantum dots. A good mask would be the one that is intact during evaporation and the surrounding area that is not covered by the mask is totally evaporated. The optimum thickness of the masking layer depends on the evaporation temperature. We have performed a series of experiments to find out the optimum AlAs mask thickness at 670°C and 690°C. Fig. 5 shows the emission peak energies at 77 K versus the lengths of thermal etching time at

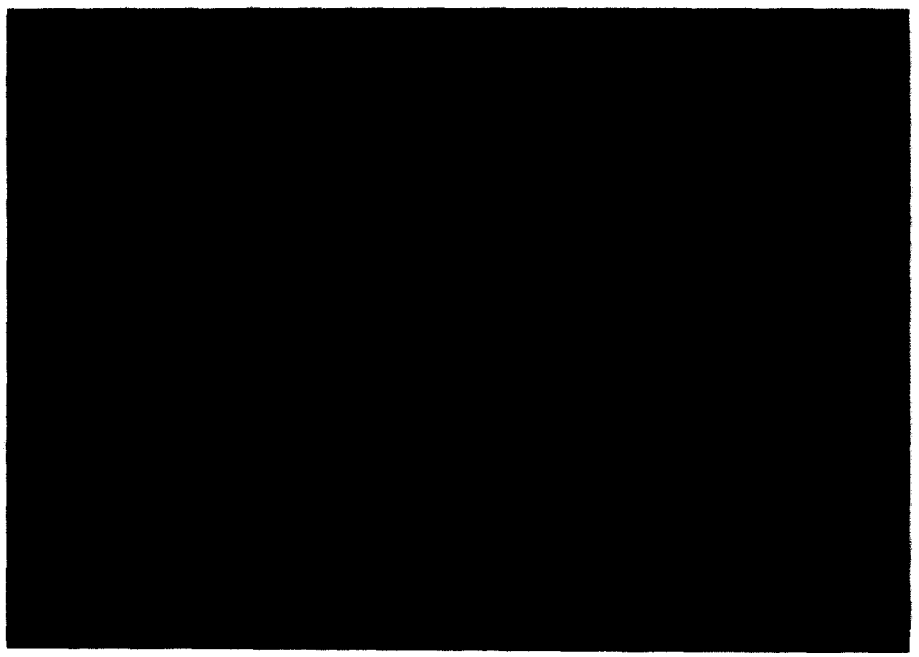

Fig. 7. The structure of the quantum dots measured by an atomic force microscope.

670°C for samples with AlAs masking layers of 0 and 0.5 ML thick. When there is no AlAs mask (0 ML), the blue shift in the emission peak is due to the uniform evaporation of the InGaAs quantum well. After it is totally evaporated, the emission peak stops at that of the GaAs quantum well. But for the sample with a 0.5 ML AlAs mask, the blue shift also stops after 1.5 min of thermal etching. The saturation energy however is lower than that of the GaAs quantum well. This is a good indication that 0.5 ML of AlAs can stand the evaporation temperature of 670°C and the InGaAs layer which is not covered by the AlAs mask has been totally etched away. At 690°C evaporation temperature, a thicker mask is needed. We have studied the behavior of InGaAs QWs with 0, 0.5, 1.0, 2.5, 3.0, 3.5 and 4.0 ML AlAs masks. Fig. 5 shows the energy of PL peaks measured at 77 K.

There are several phenomena to be noted in Fig. 6. First the emission energy for unetched QWs is higher as the AlAs layer becomes thicker. This phenomenon can be explained by the increase of the quantized energy because of the presence of the AlAs mask. When the AlAs mask is 4 ML thick, the emission energy does not change with the etching time, indicating that the InGaAs quantum well is not etched at all. When the AlAs mask is less than 3.5 ML, however, blue shift after thermal evaporation is observed indicating the etching of InGaAs. But they all saturate at the emission energy of the background GaAs quantum well. So for prolonged etching, the InGaAs layer is totally etched away and no quantum dots are formed. The ideal thickness is 3.5 ML. The energy shift stops after 1.5 min of etching, indicating that etching has completed and quantum dots are formed.

6. Direct observation of quantum dots using atomic force microscopy

The quantum dots have been imaged directly using atomic force microscopy. A sample, which was taken out from the MBE growth chamber after the quantum dots formation and before the growth of other upper layers, was scanned by a Digital Instrument Nanoscope III AFM. The image is shown in Fig. 7. Quantum islands are clearly seen in the picture. The scanned area was about 4500 by 4500 Å, and the lateral dimension of each island is around 200 Å. It is worth pointing out that the sample used for this measurement had a same thermal etching condition (3.5 monolayers of AlAs and 690°C etching temperature) as that of the sample with the PL spectrum shown in Fig. 3b. The sizes of the quantum dots observed here agree with that estimated from the PL shift. The height of the islands seen from the picture is about 40 Å, which is slightly less than the thickness of the InGaAs layer deposited. But we have to bear in mind that the diameter of the tip used in the AFM measurement is around 100 Å. The depth resolution is obviously limited for high density quantum dots, which have separations also in that order.

7. Conclusion

In conclusion, we have demonstrated that quantum dots fabricated using in situ thermal etching and regrowth by MBE have excellent optical quality and uniformity. Because the process does not require any lithographic step and external etching, damage free quantum dots can be achieved. There is no degradation in PL emission caused by non-radiative recombination centers due to surface states. Very high emission intensity is attributed to the enhanced oscillator strength for exciton recombination because of the confinement of the excitons in small quantum dots. The fabrication technique is very simple and the quantum dots can be easily incorporated in many heterostructures for device applications.

Acknowledgements

This work was supported by the National Science Council with contract number NSC83-0404-E009-092.

References

[1] Y. Miyamoto, Y. Miyake, M. Asada and Y. Suematsu, IEEE Quantum Electron. QE-25 (1989) 2001.
[2] K.T. Vahala, IEEE Quantum Electron. QE-24 (1988) 523.

[3] K. Kash, D.D. Mahoney, B.P. Van der Gaag, A.S. Gozdz, J.P. Harbison and L.T. Florez, J. Vac. Sci. Technol. B 10 (1992) 2030.
[4] H. Temkin G.J. Dolan, M.B. Panish and S.N.G. Chu, Appl. Phys. Lett. 50 (1987) 413.
[5] P.M. Petroff, J. Cibert, A.C. Gossard, G.J. Dolan and C.W. Tu, J. Vac. Sci. Technol. B 5 (1987) 1204.
[6] I.-H. Tan, R. Mirin, V. Jayaraman, S. Shi, E. Hu and J. Bowers, Appl. Phys. Lett. 61 (1992) 300.
[7] A.C. Gossard, J.H. English, P.M. Petroff, J. Cibert, G.J. Dolan and S.J. Pearton, J. Cryst. Growth 81 (1987) 101.
[8] D.C. Liu and C.P. Lee, Appl. Phys. Lett. 63 (1993) 3300.
[9] O. Brandt, L. Tapfer, K. Ploog, R. Bierwolf, M. Hohenstein, F. Phillipp, H. Lage and A. Heberle, Phys. Rev. B 44 (1991) 8043.
[10] D. Leonard, M. Krishnamurthy, C.M. Reaves, S.P. Denbaars and P.M. Petroff, Appl. Phys. Lett. 63 (1993) 3203.
[11] J.M. Moison, F. Houzay, F. Barthe, L. Leprince, E. Andre and O. Vatel, Appl. Phys. Lett. 64 (1994) 196.
[12] K. Kash, D.D. Mahoney, B.P. Van der Gaag, A.S. Gozdz, J.P. Harbison and L.T. Florez, J. Vac. Sci. Technol. B 10 (1992) 2030.
[13] H. Temkin G.J. Dolan, M.B. Panish and S.N.G. Chu, Appl. Phys. Lett. 50 (1987) 413.
[14] P.M. Petroff, J. Cibert, A.C. Gossard, G.J. Dolan and C.W. Tu, J. Vac. Sci. Technol. B 5 (1987) 1204.
[15] I.-H. Tan, R. Mirin, V. Jayaraman, S. Shi, E. Hu and J. Bowers, Appl. Phys. Lett. 61 (1992) 300.
[16] A.C. Gossard, J.H. English, P.M. Petroff, J. Cibert, G.J. Dolan and S.J. Pearton, J. Cryst. Growth 81 (1987) 101.
[17] J.H. Neave, B.A. Joyce, P.J. Dobson and N. Norton, Appl. Phys. A 31 (1983) 1.
[18] G.W. Bryant, Phys. Rev. B 37 (1988) 8763.
[19] H. Benisty, C.M. Sotomayor-Torres and C. Weisbuch, Phys. Rev. 44 (1991) 10945.
[20] K. Brunner, U. Bockelmann, G. Abstreiter, M. Walther, G. Bohm, G. Trankle and G. Weimann, Phys. Rev. Lett. 69 (1992) 3216.
[21] L. Davis, K.K. Ko, W.Q. Li, H.C. Sun, Y. Lam, T. Brock, S.W. Pang and M.J. Rooks, Appl. Phys. Lett. 62 (1993) 2766.
[22] I. Vurgaftman and J. Singh, Appl. Phys. Lett. 64 (1994) 232.